JOURNAL OF GEOPHYSICAL RESEARCH, VOL. 111, B06312, doi:10.1029/2004JB003578, 2006

Coseismic ruptures and tectonic landforms along the Düzce segment of the North Anatolian Fault Zone (Ms 7.1, November 1999)

S. Pucci,[1,2] N. Palyvos,[1] C. Zabci,[3] D. Pantosti,[1] and M. Barchi[4]

Received 15 December 2004; revised 9 January 2006; accepted 6 March 2006; published 30 June 2006.

[1] This paper presents a comparison between the pattern of surface ruptures produced by a single earthquake and patterns of cumulative deformation. We performed a detailed study of the 1999 earthquake coseismic ruptures and of the long-term tectonic landforms in a key area of the Düzce fault segment of the North Anatolian fault. We observed a scale-independent en echelon arrangement of the coseismic surface ruptures. As a whole, the long-term geomorphic expression of the Düzce Fault near the 1999 ruptures is evidence of the principal slip zone at depth that accommodates the bulk of the displacement during an individual rupture event. This may stay localized through many rupture episodes with persistent geometry and kinematics. The long-term tectonic and geomorphic expression of the fault in a broader area around the 1999 ruptures defines a wider deformation zone. In fact, an old and complex fault arrangement has been mapped, partially coinciding with the 1999 rupturing fault, suggesting that the 1999 ruptures are an incomplete expression of the long-term Düzce fault system. The relationships between the coseismic and the old fault systems suggest an evolution of the fault pattern trough time, with a tendency to simplify a geometric complexity into a straighter, mature trace. The integrated investigation of long-term tectonic morphologies and structural pattern offers a noteworthy frame to interpret the coseismic rupture kinematics and clarifies their complexities. Moreover, to fully understand the principal slip zone at depth, this work shows the importance of the study of strain distribution pattern and evolution of surface rupturing faults.

Citation: Pucci, S., N. Palyvos, C. Zabci, D. Pantosti, and M. Barchi (2006), Coseismic ruptures and tectonic landforms along the Düzce segment of the North Anatolian Fault Zone (Ms 7.1, November 1999), *J. Geophys. Res.*, *111*, B06312, doi:10.1029/2004JB003578.

1. Introduction

[2] Large earthquakes are a unique opportunity to shed light to seismogenic sources and the related tectonic processes. They provide a snapshot on the long-term tectonic processes that are controlling the evolution of the tectonic structures of a specific region. Combined observations of coseismic surface ruptures, tectonic geomorphology and earthquake geology can identify the principal deformation zones at the surface (PDZ) that, as expression of a localized slip plane at depth (PSZ, principal slip zone), can improve the understanding and characterization of seismogenic structures and of their evolution in space and time. These disciplines have developed significantly during the past 2 decades, but there is still a need for detailed case studies to cover the wide variety of tectonic/geodynamic settings, deformation rates, geological and geomorphic environments that seismogenic zones are associated with. Freshly collected observations on recent earthquake ruptures and on their geomorphic setting are therefore a critical input to improve and to develop seismogenic source models. Under this light, recent large earthquakes with sizable coseismic effects at the surface represent excellent case studies.

[3] We investigated the area struck by the 12 November 1999 Mw 7.1 earthquake that ruptured the Düzce segment of the North Anatolian Fault Zone (NAFZ) (Figures 1 and 2). This area is favorable for this type of studies because of the occurrence and preservation of the spectacular 1999 surface ruptures coupled with impressive tectonically driven landforms. Thus the Düzce fault is a natural laboratory where coseismic deformation, tectonic landforms and geological structures can be investigated and compared in order to reconstruct the fault zone history and to understand if forecasting some of the characteristics of the future earthquake rupture could be possible.

[4] In this paper we discuss the results of an investigation performed in a key area of about 70 km^2 along the central part of the Düzce fault segment (Figure 2). This area was selected because of the extensive presence of faulted Pleistocene and Holocene continental deposits that constrain timing and amount of ongoing deformation. We describe and analyze the 1999 coseismic rupture patterns along with the long-term (Late Holocene to Late Pleistocene) land-

[1]Sismologia e Tettonofisica, Istituto Nazionale di Geofisica e Vulcanologia, Rome, Italy.
[2]Also at Dipartimento di Scienze della Terra, Universita' degli Studi di Perugia, Perugia, Italy.
[3]Istanbul Technical University, Istanbul, Turkey.
[4]Dipartimento di Scienze della Terra, Universita' degli Studi di Perugia, Perugia, Italy.

0148-0227/06/2004JB003578$09.00

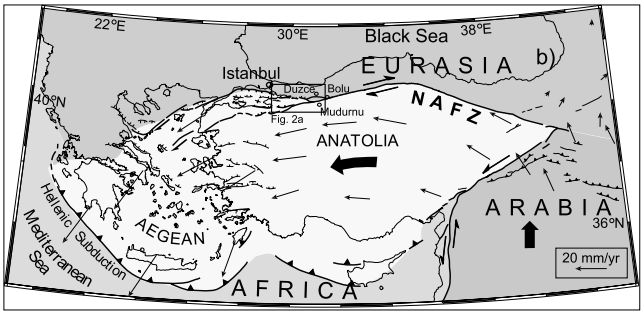

Figure 1. Tectonic setting of the eastern Mediterranean and continental extrusion of the Anatolian plate. Current motion relative to Eurasia (GPS (global positioning system) and SLR (satellite laser ranging) velocity vectors, in mm/yr, from *Reilinger et al.* [1997]) (modified from *Armijo et al.* [1999]).

forms and structures as result of cumulative fault-related deformation. Rupture style and complexity were investigated by means of field survey, structural geological analysis, and aerial photo interpretation. We carried out a detailed tracing and measurement of the 1999 ruptures, coupled with geological and geomorphological mapping at a 1:25,000 scale. Geomorphological observations were made on 1:18,000 and 1:35,000 scale aerial photographs, a 20-m-resolution Digital Elevation Model (interpolated from 1:25,000-scale topography, 10-m digital contours) and standard morphometric derivatives (hill-shaded and slope angle maps), as well as during the field survey.

[5] In the following, after a brief introduction to the tectonic framework of the North Anatolian Fault Zone, we describe (1) the patterns of the coseismic ruptures at different scales and (2) the long-term fault patterns that are derived from cumulative tectonic landforms, along the coseismic ruptures and at a broader area around them. Subsequently, we make a comparison between these two data sets, in order to understand whether their relationships reveal any space and time evolution of the fault pattern at the surface.

2. Overview on the North Anatolian Fault Zone (NAFZ)

[6] The NAFZ is an active right-lateral system, about 1500 km long, which bounds to the north the westward extruding Anatolian block [*McKenzie*, 1972; *Şengör*, 1979;

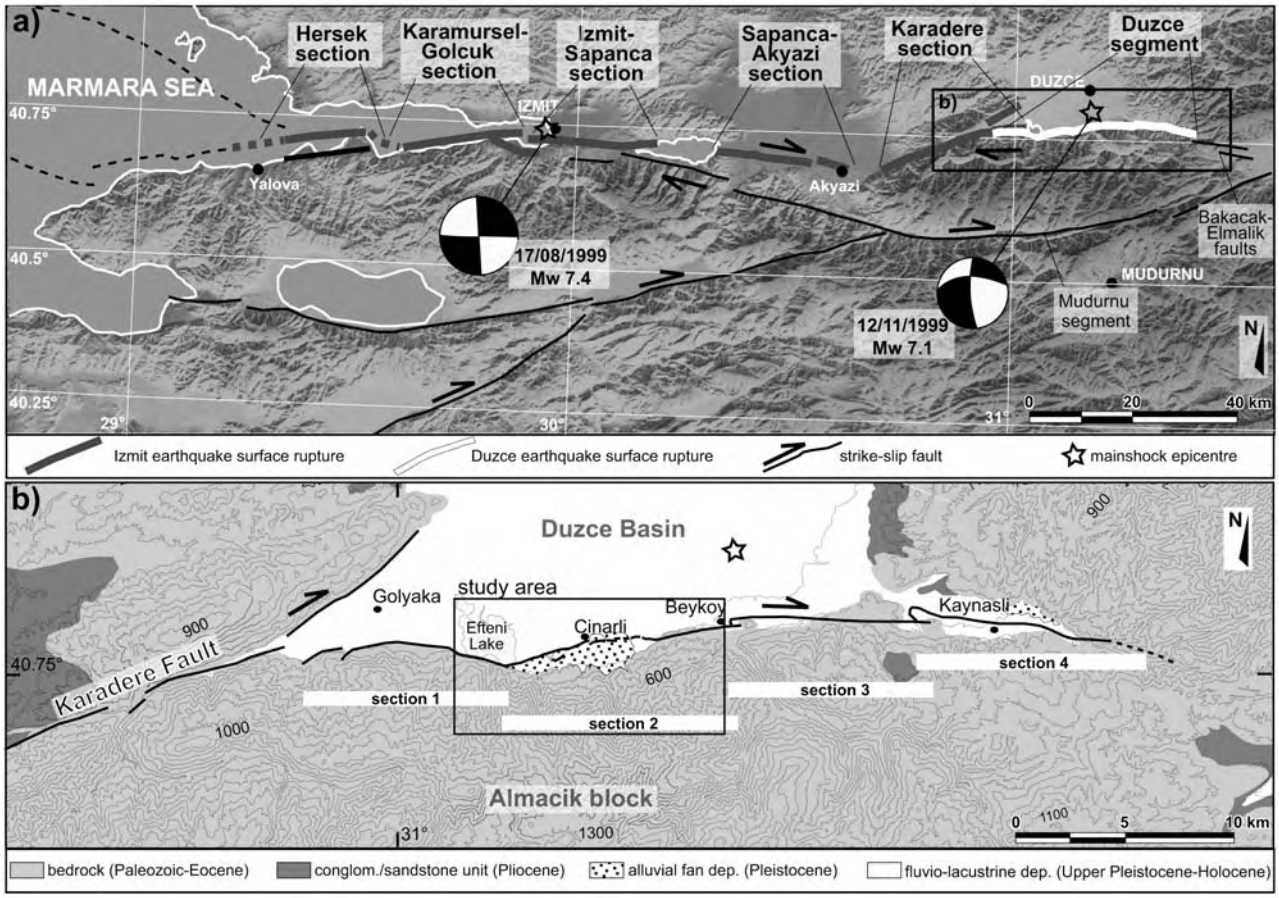

Figure 2. (a) The 1999 Izmit and Düzce earthquake. Epicentre location and focal mechanism solutions from Harvard CMT, surface rupture traces from *Akyüz et al.* [2000]. b) Simplified geological map of the Düzce area (modified from *Herece and Akay* [2003]) and trace of the Düzce fault with sections (modified from *Akyüz et al.* [2000]). Contour interval is 100 m.

Barka, 1992; *Şaroğlu et al.*, 1992] (Figure 1). Since the Middle/Late Miocene (13–5 Ma) the NAFZ has accumulated a geologic displacement on the order of 85–120 km [*Seymen*, 1975; *Sengor*, 1979; *Barka*, 1981; *Barka and Hancock*, 1984; *Westaway*, 1994; *Armijo et al.*, 1999; *Hubert-Ferrari et al.*, 2002]. This displacement translates to long-term and short-term geologic slip rate of 0.5–0.8 cm/yr [*Tokay*, 1973; *Seymen*, 1975; *Barka and Hancock*, 1984] and 1.8 cm/yr [*Hubert-Ferrari et al.*, 2002], respectively. Conversely, GPS networks measured present-day strain rates in the northern part of the Anatolian block that reach ~2–3 cm/yr [*Reilinger et al.*, 1997, 2000; *Straub et al.*, 1997; *McClusky et al.*, 2000; *Kahle et al.*, 1999, 2000].

[7] To the east of the town of Bolu (Figure 1), the NAFZ is formed by a main single trace but, west of it, it splays into two main strands, the Düzce and the Mudurnu fault segments, where GPS data indicate that the former accommodates up to 10 mm/yr [*Ayhan et al.*, 1999]. Farther west (Figure 2a), the NAFZ splays again into three major strands and the northernmost one is considered to accommodate most of the present-day strain [*Barka and Kadinski-Cade*, 1988; *Straub et al.*, 1997].

[8] The number of large, historical earthquakes attributed to the NAFZ testifies that the present-day high strain rate is seismically accommodated and places this fault among the most active strike-slip faults worldwide [*Ambraseys*, 1970; *Ambraseys and Finkel*, 1995; *Ambraseys*, 2002]. Seismicity along the active segments of the NAFZ is characterized by frequent moderate to large earthquakes ($M > 7$) with focal mechanisms that show essentially pure right-lateral strike-slip solutions [*Canitez and Ucer*, 1967; *McKenzie*, 1972] (see also Reinecker et al., 2004 release of the World Stress Map, available at http://www.world-stress-map.org).

[9] The 1999 earthquakes are the most recent occurring on the NAFZ in the 20th century. The first of these earthquakes occurred on 17 August and struck the Izmit region, west of the Marmara Sea. This Mw 7.4 (USGS) earthquake nucleated at a depth of 13 km and its focal mechanism (Harvard CMT) is consistent with right-lateral movement along an E-W strike-slip fault (Figure 2a). Maximum surface dextral offsets exceeded 5 m and surface rupture extended along the fault for a total rupture length of ~110 km [*Barka*, 1999; *Barka et al.*, 2000, 2002]. Three months later, on 12 November [*Muller et al.*, 2003; *Utkucu et al.*, 2003], the Mw 7.1 Düzce earthquake (USGS, KOERI) occurred. The focal mechanism solution shows almost pure, dextral strike-slip movement on an E-W nodal plane, dipping 54° to 64° to the north, with rake between 177° and 167° (USGS, Harvard CMT [*Tibi et al.*, 2001]) (Figure 2a). The pattern of aftershocks, recorded between 12 November 1999 and 20 November 1999 by the TÜBİTAK-MAM local network, is organized in clusters that are all located north of the surface trace of the Düzce fault [*Özalaybey et al.*, 2000; *Milkereit et al.*, 2000; *Cakir et al.*, 2003]. This earthquake produced right-lateral surface ruptures for a total length of ~40 km and a maximum dextral offset of 5 m [*Akyüz et al.*, 2000, 2002].

3. Düzce Fault Segment of the NAFZ

[10] The Düzce fault segment has an average E-W trend and a clear geomorphic expression for about 35 km. It separates the Quaternary Düzce and Kaynasli basins to the north from the Paleozoic-Eocene formations of the Almacik block to the south (Figure 2b) and, overall, produces uplift of the range front to the south, with respect to the plain to the north. In the western part of the basin, the E-W Düzce fault splays out from the NE-SW trending Karadere section, that ruptured during the 1999 August earthquake. The eastern termination of the Düzce fault is not clearly defined and, according to A. A. Barka and M. Erdik (unpublished report, 1993), it may join the eastern single trace of the NAFZ via a right-releasing step-over, involving the WNW-ESE trending Bakacak and Elmalik faults (Figure 2a).

[11] In general, the 40-km-long coseismic rupture is simple and narrow with a deformation zone 0.5 to 5 m wide with local exceptions where the width reaches 50 m. The coseismic ruptures do not exactly run at the mountain-piedmont interface, but affect both basin infill deposits and bedrock with a slightly northward convex trajectory. Owing to the strike variability of the rupture, transpressional and transtensional structures formed along the fault trace [*Akyüz et al.*, 2002; *Hartleb et al.*, 2002] (Figure 2b). On the basis of geometry and the coseismic slip distribution, *Akyüz et al.* [2002] divided the entire Düzce rupture into four sections (Figure 2b), each of them showing a symmetric slip tapering off toward both ends. The westernmost sections (1 and 2, Figure 2b) are separated by a releasing bend with a significant normal component of displacement, whereas the eastern sections (2, 3, and 4, Figure 2b) are separated by two 1-km wide, transpressional left step-overs. The area investigated in this paper includes the two westernmost sections of the fault, where the 1999 coseismic ruptures enter the Düzce basin and affect Quaternary continental deposits of key importance to record the cumulative fault-related deformations (Figure 3).

4. Expression of the Düzce Fault

4.1. Coseismic Expression of the Düzce Fault

[12] We mapped in detail the 1999 earthquake ruptures between Efteni Lake and Beykoy (Figure 3) and collected data on: (1) structural patterns of fractures and faults; (2) geomorphic modifications induced by the earthquake; and (3) coseismic offset of items such as roads, fences, tree lines, channels, streams, buildings, etc. (~80 new measurements, additional to those made by *Akyüz et al.* [2000, 2002] soon after the earthquake, see Tables 1 and 2). The offset measurements were collected putting attention in separating single from multiple slip events. The 1999 offsets were mostly measured using recent manufacts that were crosscut by the still visible ruptures. These manufacts provide reliable piercing points for both horizontal and vertical offsets. We measured vertical displacements on the 1999 free face at locations where we could exclude the possibility of apparent vertical displacements due to juxtaposition of topographic features (i.e., locations where the ground surface was flat or regularly sloping, without undulations). Landslides and gravitational movements occurring where the coseismic rupture crossed steep, instable slopes (Figure 3) were also carefully mapped to avoid the inclusion of surface ruptures caused by gravitational collapse in the coseismic slip measurements.

[13] On the basis of sharp changes in the strike direction of the coseismic ruptures, the fault trace, in the study area, can be

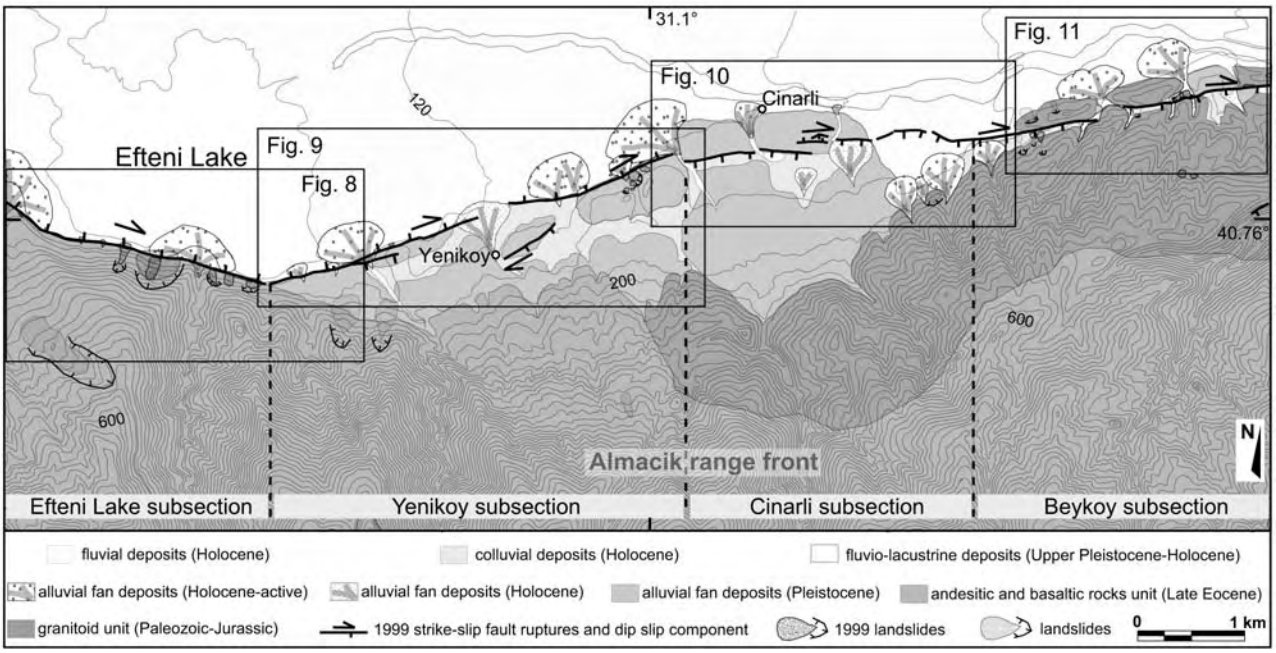

Figure 3. Geological map of the study area. Continental deposits and coseismic fault trace is from 1:25.000 scale field survey; bedrock formations are from *Herece and Akay* [2003]. Rectangle defines the location of Figures 8–11. Contour interval is 20 m.

divided into four 3- to 4-km-long subsections. These are named from west to east: the Lake Efteni, Yenikoy, Cinarli, and Beykoy subsections that trend WNW-ESE, WSW-ENE, E-W and WSW-ENE, respectively (Figure 4a). Even though the kinematics of the Düzce fault is dominantly strike-slip, field observations indicate the presence of widespread vertical motion, which was also observed in InSAR data [*Cakir et al.*, 2003]. The ruptures along the first two subsections produced relative subsidence of the block to the north. Conversely, the Cinarli and Beykoy subsections produced topographic offset with relative subsidence of the block to their south (Figure 4). This had impact on local north-flowing drainages, which were dammed at several points by coseismic scarps across them.

[14] Overall, the slip measurements (Figure 4b and Tables 1 and 2) exhibit a great variability along strike, with 4.5-m maximum dextral offsets (2.7-m average) and 2.5-m maximum vertical offset. The characteristics of the slip distribution are: (1) the maximum dextral offset of the Efteni Lake is higher than that of the other sections, (2) the average dextral offset of the Efteni Lake and Cinarli subsections is higher than that of the other sections, (3) the vertical component reaches its maximum along the Efteni subsection, and (4) the dip-slip direction changes at the boundary between Yenikoy and Cinarli subsections (Figure 4b). Modeled slip distribution at depth, obtained by joint inversion of GPS and InSar data, indicates a maximum right-lateral slip of more than 4 m, in the study area [*Cakir et al.*, 2003; *Burgmann et al.*, 2002]. The great variability of the strike-slip distribution with lower values points could denote losses of slip because of the anastomosing of the rupture, possibly due to scarce connection between the ruptured fault at depth and the surface ruptures (mechanical problems), or because of the plastic deformation in the unconsolidated deposits that overlay the bedrock. If we consider that the coseismic strike-slip distribution at the surface is representative of the movement along the seismogenic fault (see focal mechanism), the maximum dextral offsets, measured at the surface, would better represent the fault slip at depth. This is not true for the coseismic dip-slip at the surface, which includes local transtensional or transpressional components and may also contain an unknown component related to possible gravitational effects (i.e., sediment compaction).

[15] The expression of the 1999 coseismic ruptures is predominantly mole-track type. Each mole-track deformation zone, 5 to 15 m wide and 30 to 100 m long, is referred to here as a single displacement zone (SDZ) and is the morphological expression of a complex dextral fault zone, mainly consisting of synthetic, 1- to 10-m-long, strike-slip Riedel shears (Figure 5). These features are typical of poorly consolidated sediments (i.e., continental Quaternary deposits) that overlay a rigid bedrock (i.e., Paleozoic-Eocene bedrock), as observed by *Riedel* [1929] in analogical deformation experiments. The main characteristics of the system are an over-stepping, en echelon array of left-stepping synthetic Riedel shears (R-shears) and a right-stepping array of compressional fold axes (Figures 5b and 5c). Antithetic Riedel shears (R'-shears) are rarely observed even in the transfer zones at the R-shears step-overs. At places, where the width of the deformation zone increases, Riedel systems develop a second array of right-stepping synthetic shears (P-shears or Thrust-shears, Figure 6) that locally join or end up to the R-shears [e.g., *Tchalenko*, 1970; *Wilcox et al.*, 1973; *Naylor et al.*, 1986]. At a few sites, the zone of deformation consists not only of a set of en echelon R-shears, but also P-shears together with compressional fold axes. Here P-shears have grown and

Table 1. Raw Data of the Coseismic Horizontal Offsets

Offset Number	Dist.,[a] km	Cum. Dist.,[b] km	Horiz. Offset	Uncert. (±)	Q[c]	Measured Feature	Notes	Lon (wgs84)	Lat (wgs84)
1	0	0	0.3	0.2	3	wall		31.0279	40.7607
2	0.083	0.083	2.5	0.2	1	wall		31.0288	40.7606
3	0.262	0.345	2.5	0.2	1	stream deflection		31.0313	40.7593
4	0.042	0.387	2.5	0.2	1	stream deflection		31.0317	40.759
5	0.5	0.887	2.5				by *Akyüz et al.* [2002]	31.0371	40.7573
6	0.143	1.03	4.5	0.3	1	stream deflection		31.0398	40.7566
7	0.65	1.68	0.5	0.2	3	rupture geometry		31.046	40.755
8	0.354	2.034	2.8	0.3			by *Akyüz et al.* [2002]	31.0502	40.7554
9	0.362	2.396	3	0.3			by *Akyüz et al.* [2002]	31.0545	40.7541
10	0.253	2.649	4.5	0.3	1	stream deflection		31.0573	40.7536
11	1.05	3.699	4.1	0.2			by *Akyüz et al.* [2002]	31.0693	40.7558
13	0.358	4.057	1.5	0.2	1	stream deflection		31.0733	40.7574
14	0.156	4.213	2.15	0.3			by *Akyüz et al.* [2002]	31.0751	40.7576
15	0.486	4.699	0.5	0.2	2	quanat deflection		31.0802	40.7599
16	0.463	5.162	3	0.5			by *Akyüz et al.* [2002]	31.0856	40.7604
17	0.08	5.242	3	1	4	fence		31.0867	40.7569
18	0.053	5.295	2	0.2			by *Akyüz et al.* [2002]	31.087	40.7605
19	0.496	5.791	1.85	0.05			by *Akyüz et al.* [2002]	31.0927	40.7617
20	0.069	5.86	3.5	1	4	fence		31.0934	40.762
21	0.078	5.938	2.1	0.5	2	fence		31.0943	40.7623
22	0.051	5.989	2	0.1	1	pipeline		31.0949	40.7624
23	0.027	6.016	2.5	0.3	2	fence		31.0951	40.7625
24	0.822	6.838	2.3	0.2	1	fence		31.1046	40.7643
25	0.068	6.906	3.25	0.25			by *Akyüz et al.* [2002]	31.1054	40.7645
26	0.104	7.01	3.3	0.2	1	channel		31.1067	40.7646
27	0.089	7.099	3.1	0.2	1	fence		31.1077	40.7647
28	0.208	7.307	3.1	0.2			by *Akyüz et al.* [2002]	31.1101	40.7652
29	0.247	7.554	3.6	0.1	1	fence		31.1131	40.7652
31	0.09	7.644	3.5	0.1	1	fence		31.1143	40.7651
33	0.047	7.691	3.3	0.2	1	fence		31.1149	40.7652
34	0.039	7.73	3.75	0.25			by *Akyüz et al.* [2002]	31.1154	40.7652
35	0.357	8.087	2	0.2	1	fence		31.1197	40.7657
36	0.03	8.117	2	0.2	1	fence		31.12	40.7657
37	0.219	8.336	3	0.15			by *Akyüz et al.* [2002]	31.1226	40.7661
38	0.068	8.404	3.3	0.2	1	channel and tree line		31.1234	40.7661
39	0.73	9.134	3.8	0.3			by *Akyüz et al.* [2002]	31.1321	40.766
40	0.251	9.385	2.5	0.2	1	fence		31.1351	40.7661
41	0.132	9.517	3.35	0.1			by *Akyüz et al.* [2002]	31.1366	40.7662
42	0.091	9.608	3.3	0.1			by *Akyüz et al.* [2002]	31.1377	40.7662
43	0.155	9.763	2.75				by *Akyüz et al.* [2002]	31.1395	40.7663
44	0.955	10.718	2	0.2	1	rupture geometry		31.1506	40.7682
45	0.04	10.758	1.5	0.2	1	wall		31.151	40.7684
47	0.07	10.828	1.3	0.15			by *Akyüz et al.* [2002]	31.1518	40.7683
48	0.513	11.341	3	0.2	1	stream deflection		31.1579	40.7691
49	0.036	11.377	4	0.5			by *Akyüz et al.* [2002]	31.1583	40.7692
50	0.047	11.424	2.8	0.2	1	fence		31.1589	40.7693
51	0.096	11.52	2.5	0.3	1	stream deflection		31.1599	40.7694
52	0.118	11.638	1.5				by *Akyüz et al.* [2002]	31.1613	40.7695
53	0.083	11.721	1.2	0.2	1	fence		31.1623	40.7697
54	0.198	11.919	2.5	0.2			by *Akyüz et al.* [2002]	31.1646	40.7698
55	0.045	11.964	2.7	0.2	2	fence		31.1652	40.7699
57	0.194	12.158	2.2	0.2	1	fence		31.1675	40.77
58	0.272	12.43	0.15				by *Akyüz et al.* [2002]	31.1708	40.7704
59	0.02	12.45	3.7	0.35			by *Akyüz et al.* [2002]	31.1723	40.764
60	0.053	12.503	3	0.5	3	fence		31.1716	40.7705
61	0.03	12.533	2.7	0.2			by *Akyüz et al.* [2002]	31.1719	40.7706

[a]Distance from the previous measured offset.
[b]Cumulative distance from the western tip.
[c]Data quality (Q, 1 high, 4 low).

linked to R-shears, forming shear lenses, and afterward Y-shears have also developed, in a typical anastomosing pattern of a through-going wrench fault, parallel to the SDZ [e.g., *Woodcock and Schubert*, 1994; *Naylor et al.*, 1986] (Figure 6). Locally, arrays of fractures form as well, with a prevalent extensional kinematics (T-fractures).

[16] At smaller scale, the 30- to 100-m-long SDZs themselves are also organized in slightly overlapping en echelon arrays. At this scale the SDZs constitute a left-stepping synthetic Riedel system spaced 3 to 20 m, which shows a clear continuity for a length of 300 to 800 m. The envelope of this en echelon array defines a principal displacement

Table 2. Raw Data of the Coseismic Vertical Offsets

Offset Number	Dist.,[a] km	Cum. Dist.,[b] km	Vertical Offset	Uncert. (±)	D. side[c]	Q[d]	Measured Feature	Notes	Lon (wgs84)	Lat (wgs84)
1	0	0	1	0.2	N	2	wall		31.028	40.7607
2	0.034	0.034	2.5	0.1	N	1	rupture		31.0283	40.7606
5	0.025	0.059	2.5	0.1	N	1	rupture		31.0286	40.7604
8	0.037	0.096	2.5	0.1	N	1	rupture		31.0292	40.7604
11	0.028	0.124	2.5	0.1	N	1	rupture		31.0294	40.7603
13	0.108	0.232	2.1	0.4	N-S			by *Akyüz et al.* [2002]	31.0306	40.7598
15	0.282	0.514	1.5	0.1	N	1	rupture		31.0334	40.7583
16	0.209	0.723	1.5	0.1	N	1	rupture		31.0357	40.7578
17	0.136	0.859	0.7		N			by *Akyüz et al.* [2002]	31.0373	40.7574
18	0.262	1.121	2	0.2	N	2	rupture	landslide	31.0402	40.7565
19	0.284	1.405	1.9	0.1	N			by *Akyüz et al.* [2002]	31.0437	40.7565
20	0.267	1.672	1	0.2	N	2	rupture	landslide	31.0464	40.7549
21	0.314	1.986	2		N			by *Akyüz et al.* [2002]	31.0503	40.7555
22	0.386	2.372	2		N			by *Akyüz et al.* [2002]	31.0546	40.7543
23	0.53	2.902	1.5	0.1	N	1	rupture		31.0606	40.7543
24	0.672	3.574	0.5	0.1	S	1	rupture		31.0683	40.7558
25	0.27	3.844	0.5	0.1	N	1	rupture		31.0713	40.7569
26	0.337	4.181	0.35		N			by *Akyüz et al.* [2002]	31.0751	40.7577
27	0.193	4.374	1	0.1	N	1	rupture		31.0772	40.7583
28	0.127	4.501	1	0.1	N	1	rupture		31.0786	40.7588
29	0.147	4.648	1.3	0.2	N	1	rupture		31.0802	40.7594
31	0.083	4.731	1	0.1	N	1	rupture		31.0813	40.7592
34	1.21	5.941	1	0.2	N	1	rupture	landslide	31.0949	40.7625
35	1.091	7.032	0.4	0.2	S	2	rupture		31.1074	40.765
36	0.472	7.504	2	0.2	S	2	rupture		31.113	40.7653
39	0.093	7.597	1.6	0.2	S	1	rupture		31.1141	40.7651
41	0.246	7.843	0.7	0.1	N	1	rupture		31.1171	40.7655
42	1.219	9.062	1	0.1	S	1	rupture		31.1315	40.7664
43	0.282	9.344	0.5	0.1	N	1	rupture		31.1349	40.7661
44	0.416	9.76	1.2	0.1	S	1	rupture		31.1398	40.7664
46	0.72	10.48	1	0.1	S	1	rupture		31.1482	40.7675
47	0.11	10.59	0.6	0.1	S	1	rupture		31.1494	40.7678
48	0.073	10.663	1.2	0.1	S	1	rupture		31.1502	40.768
49	0.068	10.731	1.3	0.1	S	1	rupture		31.151	40.768
51	0.165	10.896	1.8	0.1	N	1	rupture		31.153	40.7685
53	0.101	10.997	1.4	0.1	S	1	rupture		31.154	40.7677
55	0.138	11.135	2	0.1	S	1	rupture		31.1559	40.7687
56	0.194	11.329	0	0.4	SE	1	rupture	horst 4 m high	31.1581	40.7693
57	0.349	11.678	0.2	0.1	S	1	rupture		31.1623	40.7697
58	0.114	11.792	1.5	0.2	S	1	rupture		31.1637	40.7698
59	0.314	12.106	0.9	0.1	N	1	rupture		31.1674	40.7701
60	0.197	12.303	1	0.1	S	1	rupture		31.1697	40.7703
61	0.179	12.482	1	0	S	1	rupture		31.1718	40.7705

[a]Distance from the previous measured offset.
[b]Cumulative distance from the western tip.
[c]Downthrown side (N, S).
[d]Data quality (Q, 1 high, 4 low).

zone (PDZ) that has a strike direction diverging 5°–10° from the SDZ and produces a consistent topographic offset with the uplift of one of the fault blocks (Figure 7). The alignment of the PDZs defines the average location, strike and relative movement of the 1999 surface fault trace of each subsection of Figure 4a in which it is located.

4.2. Long-Term Expression of the Düzce Fault

[17] As already mentioned, one of the reasons for selecting the study area was the fact that the 1999 ruptures affected Holocene and Pleistocene deposits. Because of this, the Quaternary deformational history of the Düzce fault can be reconstructed by investigating the setting of their depositional and tectonic landforms. In fact, the generally loose and soft recent deposits can develop well-expressed tectonic morphologies that record persistent landform modification due to faulting. Following this perspective and with the aim of highlighting the long-term tectonic setting and evolution of this part of the Düzce fault, we conducted geomorphic analysis, first along the 1999 rupture zone (hereinafter referred as near-fault), then in a broader area around it (hereinafter referred as far-field).

[18] The contribution of gravitational movements to the landform evolution and to the observed relief was considered with particular attention. Frequently, landslides are responsible for the degradation of the tectonic landforms (e.g., interrupting the continuity of fault escarpments). Most of the landslides, both old and generated by the 1999 earthquake, are located along the fault-related topographical anomalies testifying that, in the study area, the slope evolution is strongly linked to tectonics.

4.2.1. Tectonic Landforms in the Near-Fault

[19] In the following section, we discuss the geomorphological expression of the four subsections inferred from the coseismic ruptures (see previous section). This subdivision appears, in fact, to fit also the long-term fault trace, since each subsection is associated with homogeneous tectonic

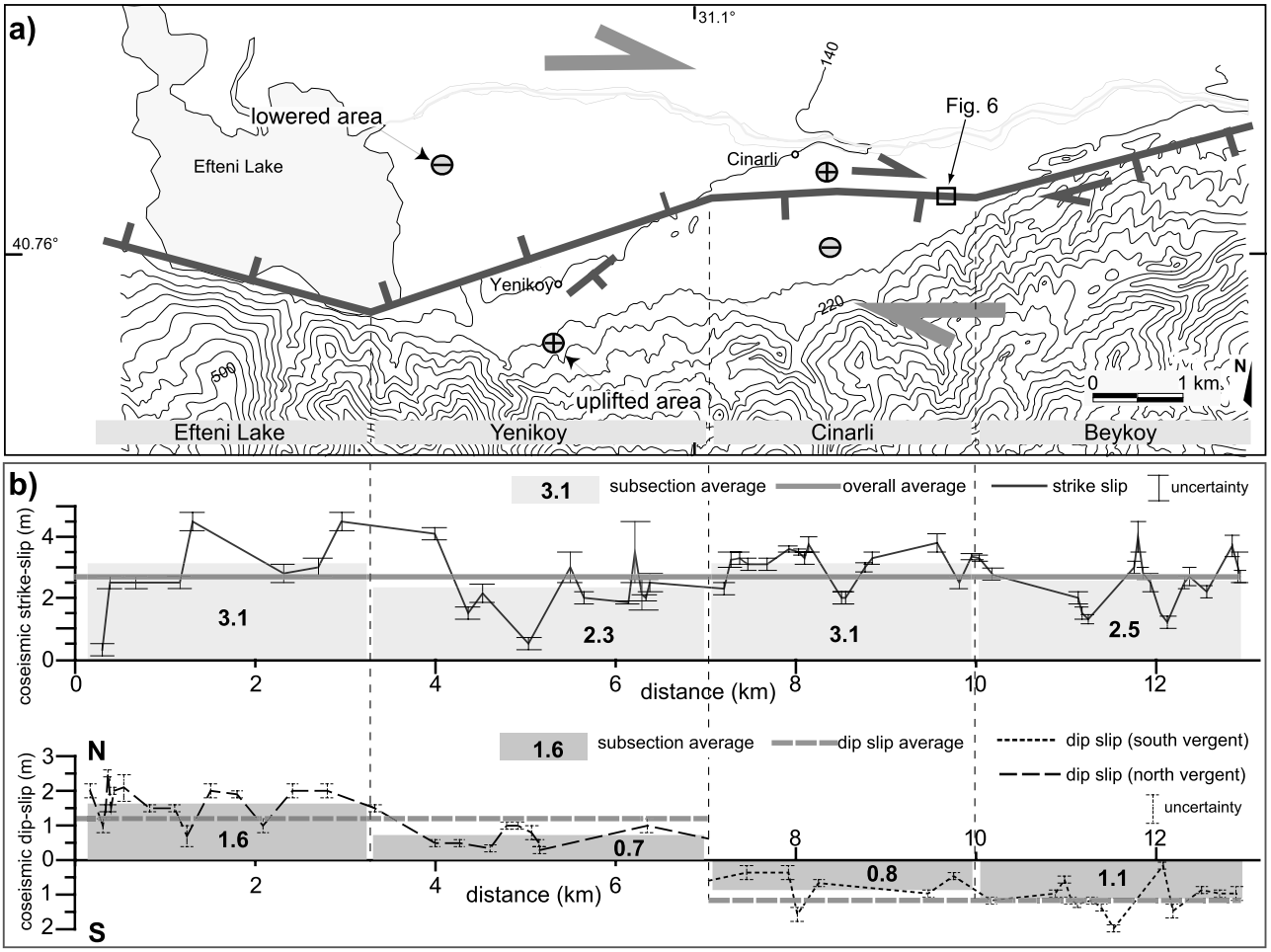

Figure 4. (a) Simplified coseismic fault trace, subdivided into the four subsections on the basis of their strike with respect to the mean strike of the Düzce fault. Contour interval is 40 m. (b) Horizontal and vertical slip distribution along the coseismic fault trace in the study area. Uncertainties have been evaluated by measuring minimum and maximum of the displacement and their range depends on the type of piercing point used.

landform assemblages that are clearly distinct from those of the adjacent subsections.

[20] The 1999 ruptures of the Efteni Lake subsection (Figure 3) coincide with the base of a steep stretch of the Almacik rangefront, and is characterized by the lack of well-developed piedmont deposits. NNE-facing triangular facets (Figure 8) are present along the range, deeply incised by canyons that exhibit hanging terraces at their outlet (x and y in Figure 8a). This setting is clearly indicative of a narrow fault zone (PDZ) located at the base of the range front that is characterized by an important and persistent NNE-trending dip-slip component.

[21] The trace of the Yenikoy subsection (Figure 3) coincides with the northward limit of a composite Pleistocene bajada (i.e., alluvial fans merging into a single apron of sediments that covers the foot of the range), but also active Holocene fans, deposited in subsequent incisions of the Pleistocene fan surface (Figure 3). This bajada has a topographic profile with a steep fanhead characterized by an abrupt transition to the fluvio-lacustrine deposits of the Düzce plain, indicating that the bajada is no longer related to the present dynamics of the latter. The generally linear contact between the bajada and the plain, is a c.a. SW-NE degraded and indented escarpment. The presence of this escarpment suggests relative subsidence north of the Düzce fault, a fact further indicated by the stream incisions across the bajada. The morphology of the bajada-bounding escarpment is not simple in its details owing to dissection by north-flowing drainages, but in general it can be subdivided into two main right-stepping elements. The westernmost is a fairly continuous, about 10-m-high, escarpment (from y to z in Figure 9) that is up to 20 m high in its central part. The eastern section is a substantially higher scarp averaging 15 m that is more degraded to the west where is perceptible only as a linear slope gradient variation. This becomes very prominent to the east (from k to w in Figure 9) where it rises up to 50 m above the Düzce plain (x in Figure 9). The right step-over, recognized in the escarpment, is also illustrated vividly by morphologic ridges along the two distinct stretches. These ridges, 300 to 1000 m long and 10 to 40 m high, have elongated shapes with long axes paralleling the escarpment elements they are associated with. The ridges have asymmetric cross profiles, with steep northern flanks and gentle south flanks, that express a smooth (ridges 1 and

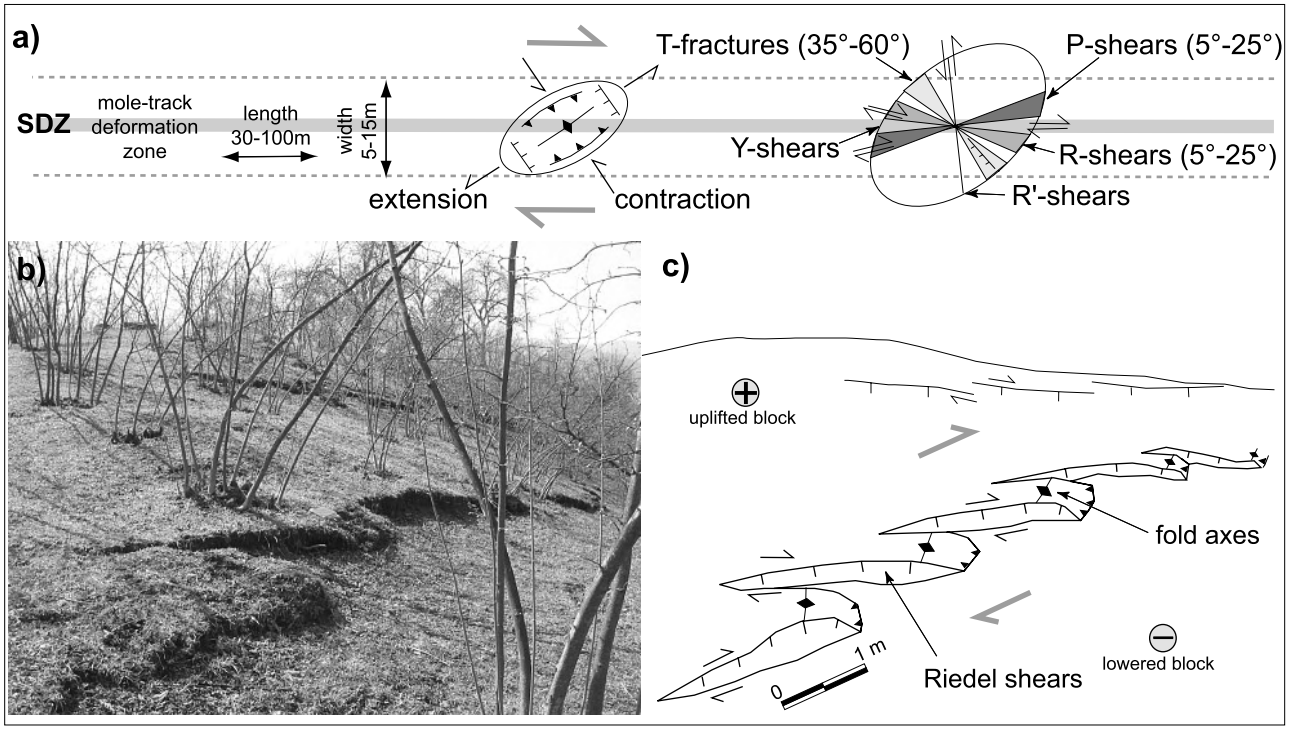

Figure 5. (a) Sketch of typical dextral single displacement zone (SDZ) and its approximate size. Outcrop scale structural elements are drawn along with the relative angle of deviation from the SDZ. (b, c) Oblique photo and sketch of a single displacement zone (SDZ) in the study area.

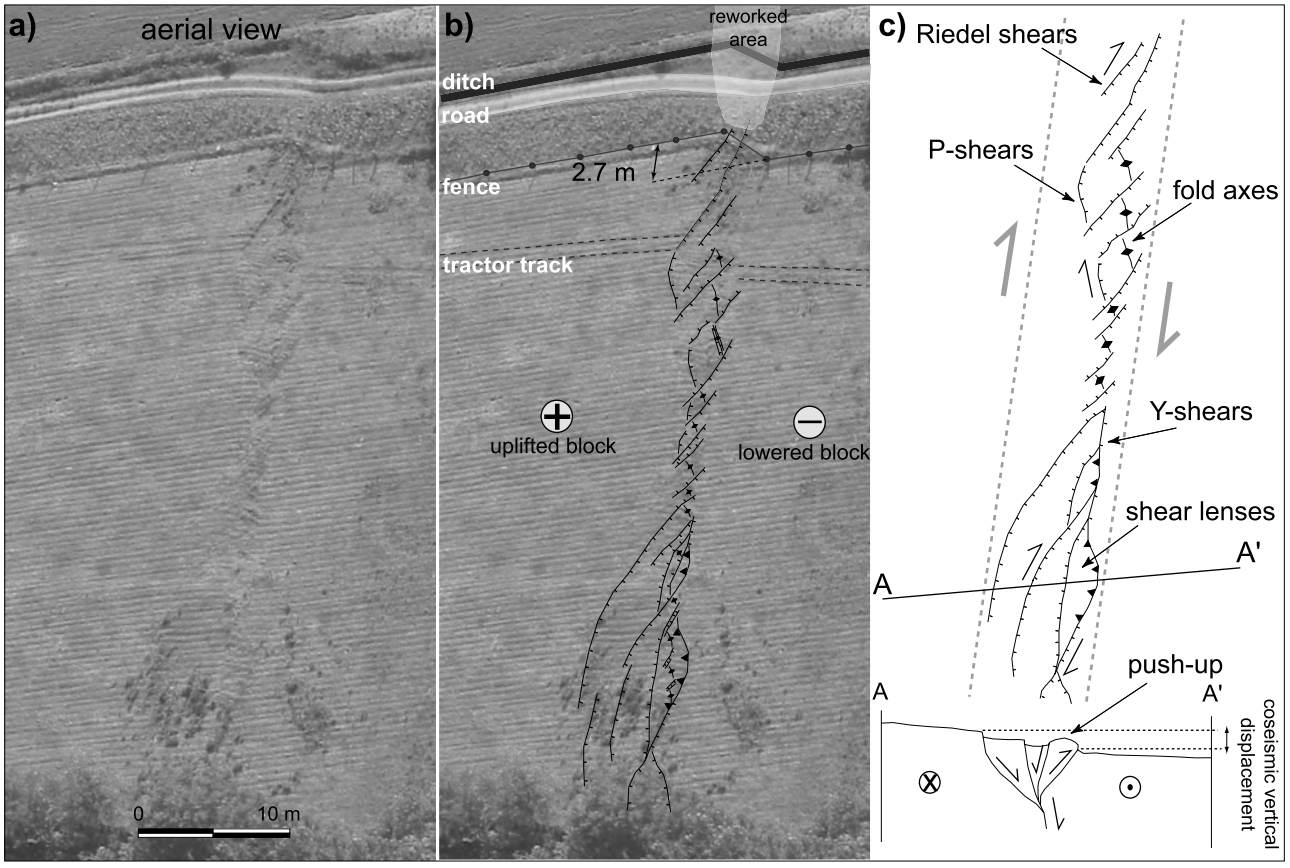

Figure 6. (a, b) Aerial view of typical anastomosing pattern of a single displacement zone (SDZ) and (c) simplified sketch map, coupled with not-in-scale topographic profile (see Figure 4 for location).

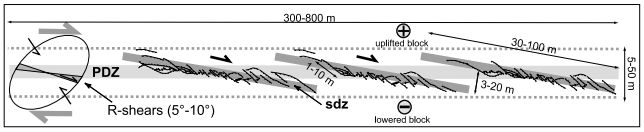

Figure 7. Sketch of the en echelon arrays formed by single displacement zones (SDZ), whose envelope represents a principal displacement zone (PDZ). Note the approximate size in relation to Figure 5.

2 in Figure 9) or abrupt (ridges 3 and 4 in Figure 9 and see profile A-A′ in inset) transition to the bajada surface. These observations suggest that the Yenikoy subsection is formed by two main, ~500 m spaced, WSW-ENE striking, ~2-km-long right-stepping fault traces (y-z and k-w in Figure 9) that have been producing uplift of the block to their south.

[22] The Cinarli subsection is associated with a prominent, 3 to 15 m high, south-facing escarpment across the bajada deposits (Figure 3 and Figure 10b). This ~E-W trending escarpment is formed by left-stepping en echelon, 200- to 700-m-long and ~100-m-spaced scarps and constitutes the northern boundary of a flat and depressed area. The escarpment has a topographic profile characterized by a sharp asymmetric warp: A steep and short southern slope contrasts with a gentle northern slope, whose gradient is coincident with the bajada depositional gradient (see profile B-B′ in inset of Figures 10a and 10b). In some cases, the scarps of the Cinarli subsection act as natural dams for northward flowing drainages, being thus responsible for the formation of ponds, flooding and alluvial deposition. The major dammed areas are drained by large artificial channels (Figure 10a). In the easternmost part of the subsection, two escarpment-bounded depressions also trap Holocene pond and fan deposits against the scarp (x in Figure 10a). North-flowing drainages are characteristically deflected in an apparent left-lateral sense, since they cross the bajada through the escarpment step-overs, where the damming is less effective (i.e., the scarps are less high where they overlap; Figure 10a). The complex setting described above is suggestive of a set of short, up to 1-km-long left-stepping fault strands forming the Cinarli subsection that have been producing subsidence of the southern block.

[23] Farther east, the Beykoy subsection contrasts with the Cinarli subsection because it is associated with well-expressed, 400- to 800-m-long, WSW-ENE trending elongated tectonic ridges, along the base of the range front (Figures 3 and 11). Most of these ridges are made of a Paleozoic-Jurassic granitoid unit, are ~70 m high and have symmetric profiles and steep slopes (Figure 11b). Only one of the eastern ridge is made of recent deposits of a remnant of a Holocene bajada. Compared to the bedrock ridges, it is lower (15 m high) and asymmetric, with a steep south-facing slope. Narrow and hanging WSW-ENE linear valleys, up to 40 m deep, have developed between the elongated ridges and the base of the range front. The north-flowing drainages show clear anomalies. Right-hand stream deflections of about 100 m (x in Figure 11a) occurred because of: the growth and offset of the ridges that act as natural dams to their flow; incision of both linear valleys and ridges that forced the streams to maintain their bed; and low stream power not enough to erode and to straighten their course. Tectonic influence on drainage patterns is also expressed by stream piracy along the fault (creating apparent sinistral deflections) and perched ponding areas (y and z, respectively in Figure 11). The setting of the Beykoy section suggests the existence of a WSW-ENE striking, persistent fault trace, located along the linear valley between the ridges and the range-front slope. A secondary parallel fault trace possibly bounds the northern side of the linear ridges, causing its relative uplift with respect to the Düzce plain.

4.2.2. Tectonic Landforms in the Far Field

[24] In this section, we enlarge the area of observation, from the near-fault features to a zone a few kilometers wide (Figure 12). In this broader view the long-term geomorphic characteristics of the Düzce fault, east of Lake Efteni subsection, indicates that the zone of deformation that separates the Almacik block from the Düzce plain is composed, besides the PDZ, of a complex WNW-ESE and SW-NE range front fault system (hereinafter referred to as RFS) (Figure 13a).

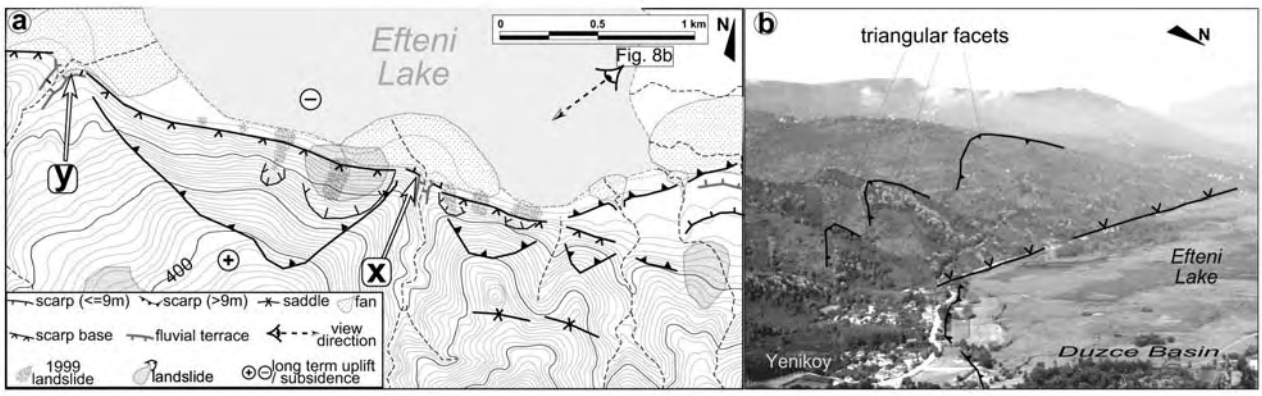

Figure 8. Cumulative tectonic landforms along the 1999 rupture subsections (see Figure 3 for location). (a) Main tectonic and geomorphological features of the Efteni Lake subsection (see text for explanation). Contour interval is 10 m. (b) Picture of the triangular facets of the Efteni Lake subsection (see Figure 8a for view location).

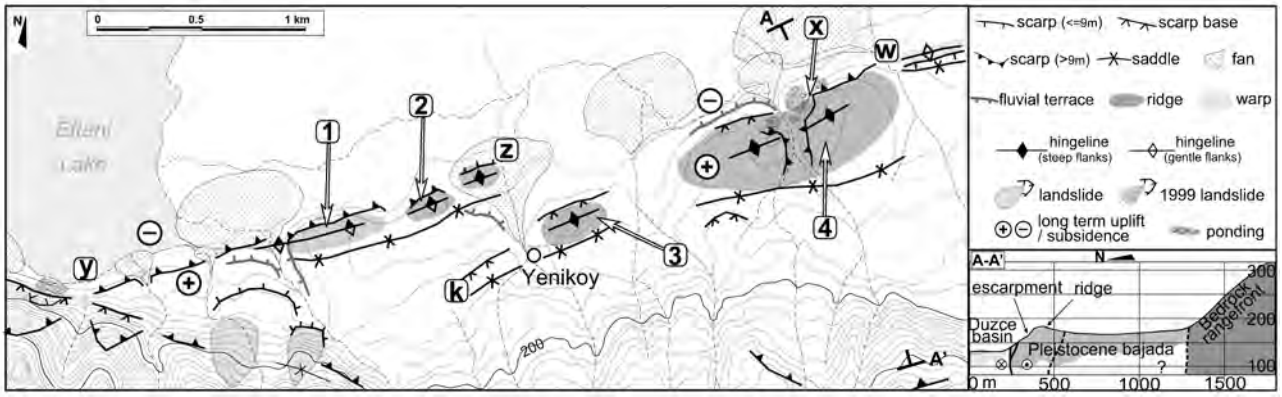

Figure 9. Cumulative tectonic landforms along the Yenikoy subsection (see Figure 3 for location and see text for explanation) and main tectonic and geomorphological features of the Yenikoy subsection (see text for explanation). Contour interval is 10 m. The inset shows a simplified cross section of the long-term escarpment on the Pleistocene bajada deposits that was affected by the 1999 ruptures.

[25] The Pleistocene bajada is certainly the most significant geomorphic feature highlighting this fault system (Figure 3). It developed within a ~2.5-km-wide and 7-km-long (b-c-d-f in Figure 12) fault-controlled triangular embayment of the Almacik range front. In Figure 12, stretch b-f-g of the RFS is essentially the extension towards the ESE of the Lake Efteni fault subsection. In fact, the alignments of linear ridges, valleys (y in Figure 12) and bases of indented and fairly well preserved facets, up to 250 m high (x in Figure 12), eloquently depict a tectonic boundary. This tectonic boundary is exposed in one outcrop (z in Figure 12), where facet-parallel, right-lateral fault planes juxtapose Late Eocene against Paleozoic-Jurassic units (see Figure 3). The geomorphologic expression of stretch f-d of the RFS is equally clear-cut, as a SW-NE straight boundary, characterized by facet-parallel alignments and an abrupt slope gradient change, between the 500-m-high range front slopes and the lower relief in front of them (Figure 13a). This SW-NE escarpment cannot be attributed to litho-structural control, since foliation and lineation of the outcropping bedrock strike oblique to range front (Figure 12). In addition, we observed SW-NE trending fault planes in bedrock outcrops along the escarpment. Even though clear kinematic indicators could not be identified in these fault outcrops, on the basis of their orientation with respect to the Düzce fault stress field, we may infer a transpressive character for the stretch f-d of the RFS (Figure 13a). Smaller morphological discontinuities are suggestive of the presence of several minor faults inside this major embayment, bounding a sector of bedrock of intermediate elevation (1 in Figures 12 and 13a).

[26] We also found within the bedrock units evidence for a tectonic contact along the SW-NE trending strands of the RFS (g-h in Figure 13a). In general, the geomorphic expression of the g-h strand and the lack of fault-controlled recent deposition do not suggest its present activity, but we note that *Akyüz et al.* [2002] reported up to 15-cm right-lateral offset ruptures along its easternmost part (Figure 13a).

5. Discussion

5.1. Coseismic Ruptures Versus Long-Term Tectonic Landforms in the Near Fault

[27] We identify a general coherence at the scale of principal displacement zone (PDZ), both in location and relative movement, between the 1999 coseismic fault trace

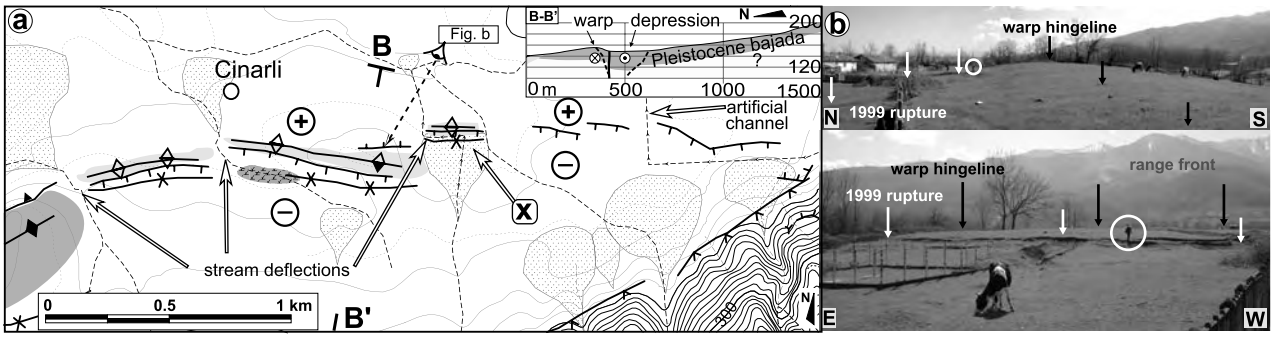

Figure 10. (a) Main tectonic and geomorphological features of the Cinarli subsection (see Figure 3 for location and see text for explanation) (legend same as Figure 9). Contour interval is 10 m. The inset shows a simplified cross section of the long-term escarpment on the Pleistocene bajada deposits that was affected by the 1999 ruptures. (b) Photos of tectonic warp (man in circle for scale) (see Figure 10a for location).

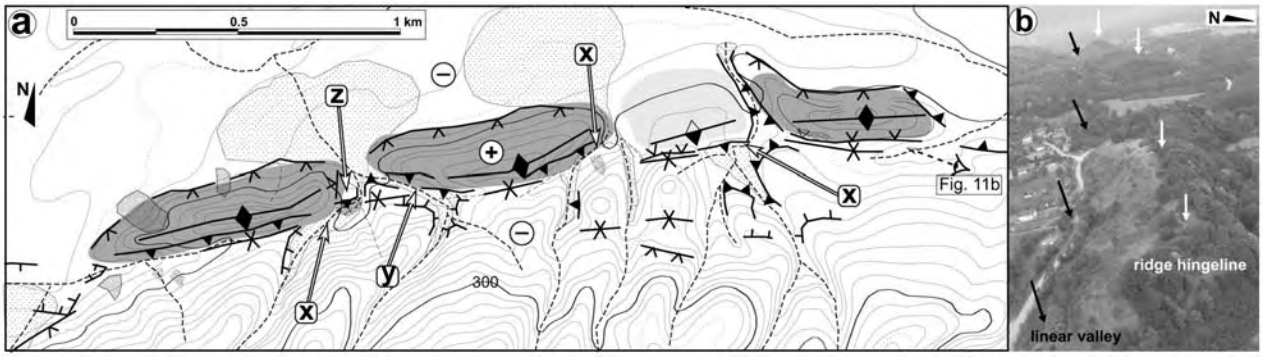

Figure 11. (a) Main tectonic and geomorphological features of the Beykoy subsection (see Figure 3 for location and see text for explanation) (legend same as Figure 9). Contour interval is 10 m. (b) Aerial view of tectonic ridges (see Figure 11a for view location).

and Holocene cumulative tectonic landforms along it (Figure 14a). The PDZ closely mimics the long-term tectono-morphologic pattern. Also, the location and distribution of the PDZ vertical component of displacement appear to correlate well with the cumulative tectonic landforms, emphasizing the preexisting relief (e.g., x in Figure 14a). On the contrary, at a larger scale (SDZ and larger, see Figure 7), the subordinate coseismic structures diverge from the long-term morphologies: the en echelon ruptures arrays generally "climb" diagonally across the landforms.

[28] The only relevant incoherences between the coseismic fault trace and cumulative tectonic landforms recognized at the scale of the PDZ are found at the Yenikoy and Cinarli subsections. In the first case, on the basis of cumulative tectonic landforms, we identify a right-step between long-term transpressive fault structure (y in Figure 14a) that was violated by two coseismic ruptures (q in Figure 14a), linking the right step-over and forming a duplex. The two, E-W trending, linkage ruptures are associated with a cumulative tectonic relief much lower than that of the two main fault stretches. This suggests that this linkage may be a secondary transfer structure, a pure strike-slip section with no vertical offset or be a late Y-shear-like feature. In the other case, along the Cinarli subsection, one of the cumulative major fault scarps was not entirely reactivated and the rupture crosscut the morphological warp linking two consecutive left stepping scarps (w in Figure 14a).

[29] The good correlation between 1999 ruptures at the PDZ scale and cumulative tectonic landforms in the near-fault indicates a persistent fault trace and style of deformation through several seismic cycles. However, apart from the Efteni Lake subsection, the 1999 ruptures represent only a part of the fault pattern inferred from cumulative tectonic landforms (and thus of the PDZ). The overall long-term deformation zone in the near-fault (Figure 14a) appears not only wider but also more complex than the coseismic one, including other fault strands to the south and/or to the north, which did not rupture in 1999. This raises the possibility that secondary structures have hosted relatively small, blind

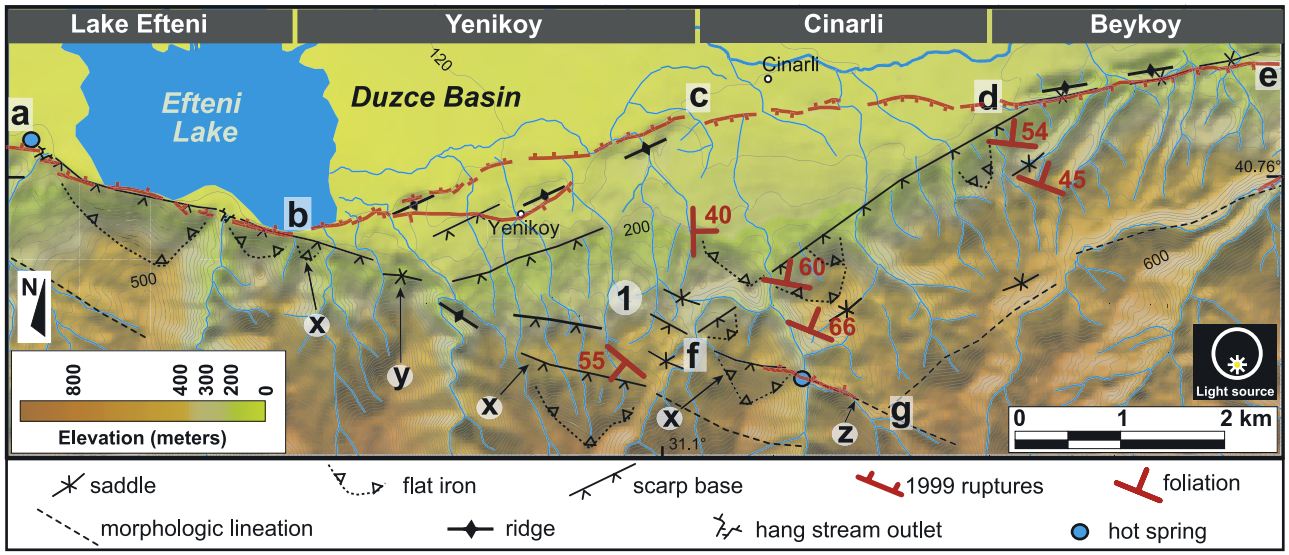

Figure 12. Broader scale tectonic geomorphology of the study area. Shaded relief is based on digital elevation model (DEM, interpolated from 10-m contours and auxiliary 5-m contours of 1:25.000 scale topographic maps) (see text for explanation). Contour interval is 20 m.

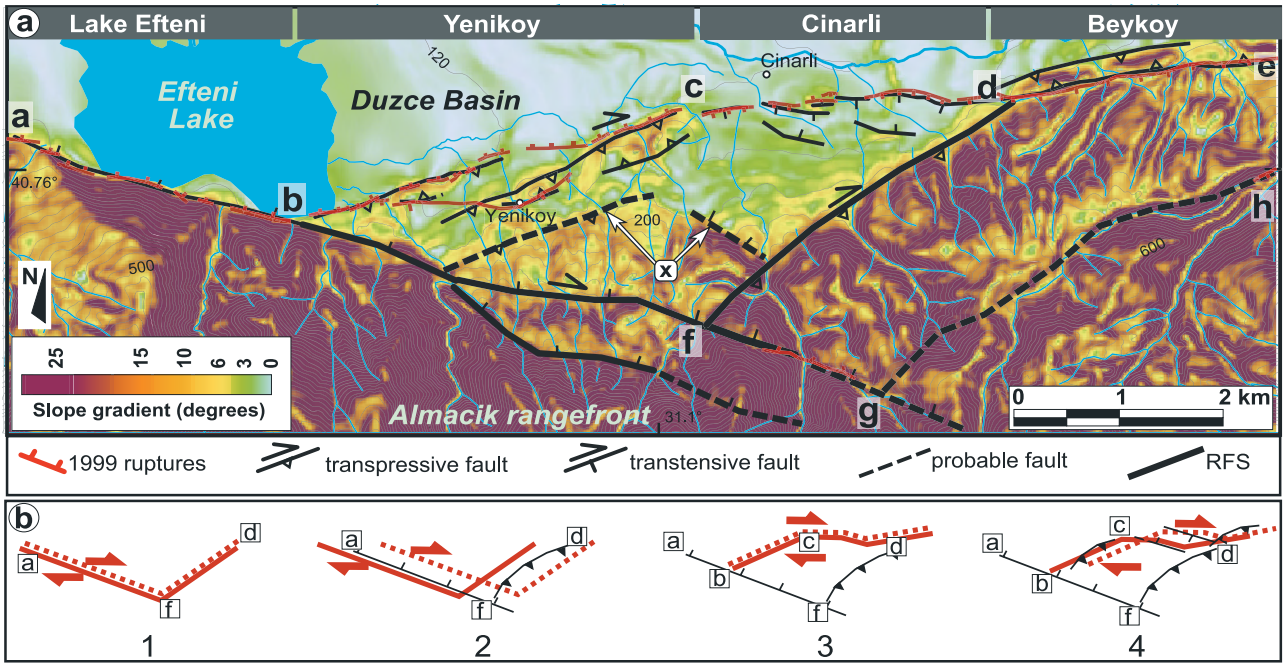

Figure 13. (a) Slope gradient map from DEM and long-term fault system of the study area. Contour interval is 20 m. (b) Schematic evolution of the Düzce fault system in the study area. Gray arrows show relative movement of the two fault sides (dashed and solid gray lines): 1, the range front faults (a-g and f-d) start to be active (Middle/Late Miocene or Late Pliocene); 2, the geometry of the range front faults produce extensional (a-f) and compressional (f-d) local stress fields (up to Early/Middle Pleistocene?); 3, the northern strand (b-c-d) starts to be active (Late Pleistocene?); and 4, the geometry of the Yenikoy (b-c) and Cinarli (c-d) subsection produce compressional and extensional local stress fields, respectively.

displacements or ruptures that only rarely reach the surface. In one case coseismic ruptures (near Yenikoy, z in Figure 14a) occurred along these secondary structures and described a PDZ up to 500 m wide. These secondary coseismic ruptures demostrates a superficial anastomosing of the fault system that contributes to the growth of tectonic landforms together with plastic deformation of loose deposits. In fact, as discussed by *Sibson* [2003], the width of the deformation zones at the surface (corresponding to PDZ in this paper) is mainly related to the presence of young cover sequences of alluvium and to free surface effects. The PDZ appears to be the surface expression of a localized slip plane at depth (hereinafter PSZ, principal slip zone; see Figure 14b), as observed along other seismogenic structures (e.g., Landers [*Sieh et al.*, 1993; *Johnson et al.*, 1994; *Lazarte et al.*, 1994]; Dast-e Bayaz [*Tchalenko and Ambraseys*, 1970; *Tchalenko and Barberian*, 1975]). This implies that measures along the 1999 surface ruptures could underestimate, although in a minor part, the total amount of the coseismic slip.

[30] Although at the outcrop scale the SDZs outline the fault location, they cannot unequivocally be indicative of the kinematics of the fault subsections. Only at a few locations, a prevalent presence of T-shears or push-ups is suggestive of transtension or transpression, respectively. In general, the mole tracks ruptures, that typify the 1999 rupture style, do not permit conclusions as to whether the relative uplift of the two fault blocks is due to a compressional or extensional component of displacement. In contrast, the cumulative tectonic landforms express clearly the local stress fields of the four fault subsections. The fault subsections reflect tectonic landforms according to strike-slip movement along an irregularly curved fault that produces transtension at releasing bends and transpression at restraining bends (Figure 14b). In fact, the E-W trend of the dextral Düzce shear couple tends to create a local transtensional strain field along Z-shaped fault trajectories and a local transpressional strain along S-shaped fault trajectories. The morphology of the Efteni lake fault subsection fits well with a normal component of the fault motion. The strike of the Yenikoy and Beykoy subsections suggests a local transpressive strain field, which is compliant with the observed right-stepping pressure ridges (the surface expression of cumulative positive flower structures).The coseismic rupture along the Beykoy subsection shows a lowering of the southern block. This displacement is most probably relative, only reflecting the growth of the pressure ridges of these subsection. This does not exclude the uplift of the Almacik block with respect to the basin as depicted by geodetic data. The Cinarli subsection shows a gentle negative flower structure, in accordance with the fact that it only slightly deviates from the average trend of the Düzce fault. This gentle flower structure affects the bajada forming local basins (Figure 14b).

[31] Summarizing, in the near-fault, the observed coseismic and long-term structures (PDZ) show vertical tectonic component that is related to local change of the fault trajectory. This geometrical complexity produces subsidiary folding and thrusting with small wavelength (less than 1 km)

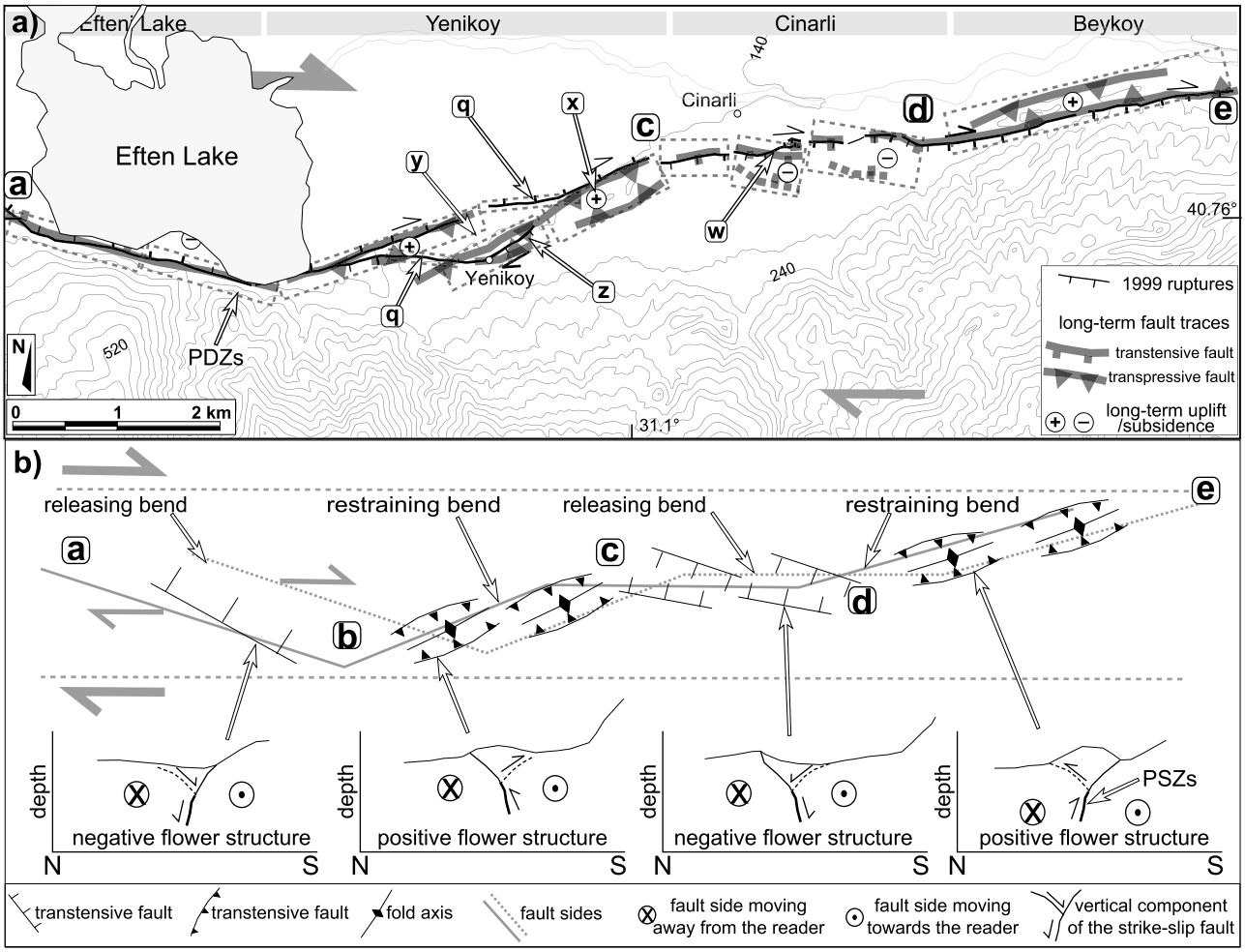

Figure 14. (a) Comparison of the 1999 coseismic ruptures and the fault trace inferred from cumulative tectonic landforms in the near-fault (see text for explanation). Contour interval is 20 m. (b) Sketch showing the coherence between restraining and releasing bends of the 1999 coseismic ruptures (a-b, b-c, c-d and d-e subsections) and the location of typical cumulative tectonic landforms. Simplified cross sections for each fault subsection are shown. Big gray arrows show the shear couple of the Düzce fault. Small gray arrows show relative movement, both coseismic and long term, of the two fault sides (dashed and solid gray lines).

that suggests they are shallow-rooted to the same master fault (PSZ from *Sibson* [2003]).

5.2. Coseismic Ruptures Versus Long-Term Tectonic Landforms in the Far Field

[32] Examining the broader area around the coseismic ruptures we have seen that, with the exception of the Efteni Lake subsection, the RFS and the 1999 fault subsections (PDZ) form a complex fault zone (hereinafter Düzce Fault System, DFS), up to 2.5 km wide (Figures 12 and 13a) that could represent the Düzce fault damage zone [*Sibson*, 2003]. The northern strand of this fault system coincides with the 1999 ruptures and associated landforms, whereas branches of the RFS bound the Pleistocene bajada to the south. Most of the 1999 coseismic ruptures in the study area traversed the Pleistocene bajada (section b-c-d), instead of taking place along the RFS (Figure 13a). No significant ground ruptures were reported following the 1999 earthquake [*Akyüz et al.*, 2002; *Hartleb et al.*, 2002], or found during our own field reconnaissance, along the RFS sections. Besides the coseismic ruptures reported by *Akyüz et al.* [2002] along the fault g-h of Figure 13a, only up to 20 cm right-lateral offset ruptures were decisively reported to us by 1999 earthquake local witnesses along 1 km of section f-g (Figures 12 and 13a). Although we cannot rule out shaking-related or sympathetic slip along preexisting fault traces that are embedded in and/or takes part to the damage zone, these observations may be suggestive also of some slip occurring in a wider area, that could contribute in the coseismic slip measurements being smaller along the main northern trace of the Yenikoy, Cinarli and Beykoy subsection (Figure 4b and strand b-c-d-e in Figure 13a).

[33] Long-term tectonic landforms along the Yenikoy and Cinarli sections suggest the persistence of the 1999 rupture complexity through several seismic cycles. However, these sections have hosted a smaller cumulative deformation and express younger morphologies with respect to the RFS. This suggests that: (1) the faults bounding the embayment to the

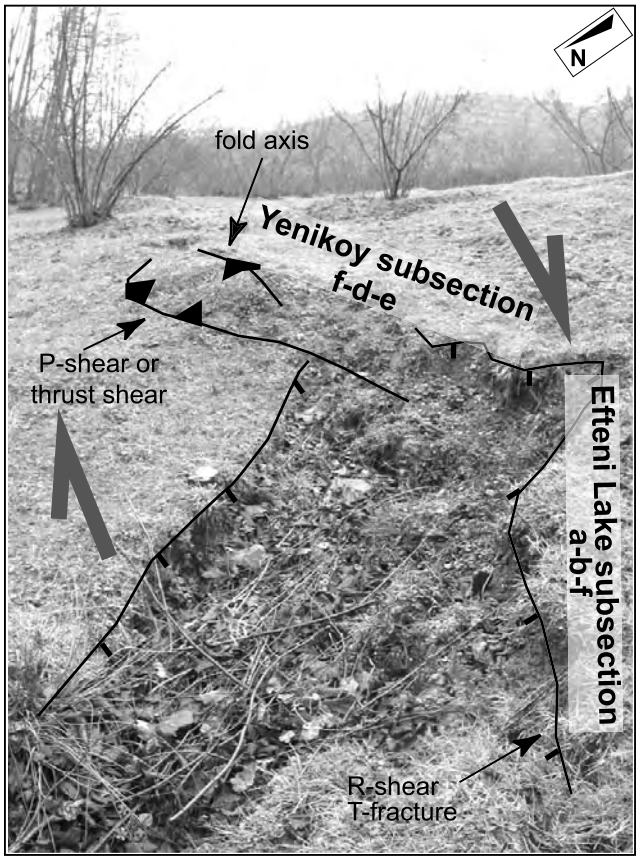

Figure 15. Detail of the 1999 surface rupture. It is noticeable that main features are scale independent analogue of both the fault pattern of two of the rupture subsections (Efteni Lake and Yenikoy subsections) and the far-field scale fault (a-b-f and f-d-e of RFS).

south (b-f-d in Figure 13a) were the principal strands of the DFS in the past (sketches 1 and 2 in Figure 13b), (2) the Yenikoy and Cinarli subsections (b-c-d) started to be active during or after the bajada deposition (sketches 3 and 4 in Figure 13b) and now accommodate most of the Düzce fault slip.

[34] The northward migration of faulting, which the interpretation above implies, translates to a tendency of the fault to simplify a major geometric complexity towards a straighter trace. This is in agreement with the combination of displacement along Riedel and P-shears that leads to the formation of Y-shears, oriented parallel to the general direction of movement [*Tchalenko*, 1970; *Woodcock and Schubert*, 1994] that is presumably a mechanically more favorable setting. The presence of the intermediate faults between the 1999 ruptures and the RFS (x in Figure 13a), that look older than the long-term landforms along the coseismic ruptures, could be suggestive of a sequence of newer fault traces stepping out from the range front with time.

[35] In summary, the broader geologic and geomorphic setting shows a kilometer-scale wide fault system (DFS) that ruptured during the 1999 earthquake in correspondence of the PDZ (Figure 13a). The DFS at the surface has been evolving through time forming the younger Yenikoy and Cinarli subsections (Figure 13b) and contributing in the growth of the damage zone. Since there are no seismic lines available and the seismologic and the geodetic data of the study area can not resolve the complexities of the near-surface and of the far-field, is not possible to determine if parts of the RFS are directly connected to the principal fault (PSZ) at depth or not. However, even though the 1999 surface ruptures suggest that most of the strain is accommodated by the northern part of the DFS (PSZ), we cannot rule out the possibility that some amount of distributed permanent shear strain also develop coseismically at depth and that other structures composing the RFS, although secondarily, participate in the deformation.

5.3. Large-Scale Versus Small-Scale Patterns

[36] The patterns of 1999 ruptures and long-term deformation exhibit essentially the same en echelon arrangement of left-stepping transtensive structures and right-stepping transpressive structures, both at meter scale and kilometer scale. Thus it is noticeable that the faults arrangement is scale independent, persisting at the SDZ, at the PDZ and at the fault subsection scales (see Figures 5, 7 and 14). Looking at the coseismic ruptures at a meter scale it is possible to observe a reduced scale analogue model of the four rupture subsections in the study area: R-shears and T-shears at releasing bends (Efteni Lake subsection); P-shears and folds at restraining bends (Yenikoy and Beykoy) (Figure 15).

[37] A similar analogy can be proposed between the coseismic meter-scale rupture pattern to the broader scale long-term fault system (RFS) depicted in Figure 13a. The a-b-f and f-d-e range front faults of the latter can be interpreted as Riedel shears and P-shears or Thrust-shears, respectively, underlined in Figure 15.

6. Conclusions

[38] The central part of the Düzce segment of the North Anatolian fault was selected to explore the relationships between the pattern of the 1999 coseismic ruptures and long-term tectonic landforms, both along the ruptures and in a broad kilometer-scale zone around them. On the basis of geometrical considerations, the coseismic rupture in the study area is divided into four kilometer-scale subsections (Figure 4). Slip distribution in part shows a distinctive pattern: The maximum right-lateral and vertical slip (4.5 m and 2.5 m, respectively) are located in the western part of the study area (Efteni lake subsection, Figure 4b); a reversal of the dip-slip orientation is located at the boundary between Yenikoy and Cinarli subsections. The coseismic surface ruptures are organized in overlapping en echelon systems that can be recognized at different scales: (1) at the outcrop scale, where 1- to 10-m-long en echelon structures define single displacement zones (SDZ, Figures 5 and 6); (2) at the hundreds-of-meters scale, with 30- to 100-m-long en echelon SDZ, forming 300- to 800-m-long principal displacement zones (PDZ, Figure 7); (3) at the kilometer scale, where also the 1999 rupture subsections, both transpressional and transtensional, are arranged in an en echelon pattern. This scale invariance of the fault pattern of 1999 ruptures and long-term deformation suggests that it is

meaningful and useful to compare natural analogues of deformation zones at different scales.

[39] On the basis of cumulative tectonic landforms we traced the long-term fault expression at the surface along the 1999 rupture zone (Figure 14). This long-term fault expression brings out that the bulk of the ongoing dextral displacement is localized mostly along the coseismic ruptures and, in addition, illustrates the existence of fault splays and a broad band of subsidiary deformation, both brittle or plastic. Because of this, the coseismic slip measured along the 1999 rupture trace could slightly underestimate the amount of seismic strain. The cumulative tectonic landforms along the 1999 rupture zone also indicate a fault pattern consistent with the coseismic one. Furthermore, they suggest different kinematics for the four coseismic subsections studied, which can be largely explained by the different orientation of each subsection with respect to the average strike of the Düzce fault. The transtensional and transpressional structures produce local vertical deformations that are characteristics of the subsections and that are related to shallow, near-surface features and do not represent the overall dip-slip component described by geodetic data or the almost pure strike-slip motion at seismogenic depth.

[40] On one hand, the geomorphic expression of the near-fault provides long-term evidence for slip localization, as observed along other active strike-slip fault zones. On the other hand, this case study shows that the width and the complexity of the surface deformation zone for the strike-slip faulting is affected by small irregularities of the fault trajectory transverse to the slip vectors, coupled with the presence and thickness of alluvial cover above the bedrock expression of the fault. Consequently, these observations draw attention to the strain partitioning between shallow transtensional and transpressional structures, above a main seismogenic structure.

[41] Cumulative tectonic landforms in the far-field zone of deformation (Figures 12 and 13a) suggest the Düzce Fault System (DFS) is complex long-term to the east of Efteni Lake subsection. This fault system is formed by: the range front fault system (RFS), WNW-ESE and SW-NE trending and bounding also a major embayment on the Almacik range front; and the PDZ represented by the WSW-ENE striking Yenikoy and Beykoy subsections and the E-W striking Cinarli subsection. Most of the coseismic ruptures and cumulative tectonic landforms (PDZ), only partially follow the RFS, but instead traverse the deposits of a Pleistocene bajada within the embayment, along the northernmost part of the long-term fault system. Overall, the DFS is formed by a PDZ as surface expression of a PSZ and by a RFS all embedded in the damage zone.

[42] The consistency between the geometry, location and style of the 1999 ruptures and the near-fault long-term tectonic landforms is a strong indication that the characteristics and complexities of the 1999 rupture in the study area have been persistent during several seismic cycles or more (Figure 14). The far-field landforms suggest that, during the Late Pleistocene, the Düzce fault developed structures forming the Yenikoy and Cinarli subsections, that abandoned the older rangefront-bounding faults. This evolution can be interpreted as a tendency of the deformation zone to simplify a complex geometry into a more straight fault trace (Figure 13b) and we expect the fault system to continue to straighten itself out in the future, until it becomes a smooth and narrow fault zone.

[43] One of the main conclusions of this study is to confirm that the comprehensive analysis of tectonic landforms and associated structures is a valuable tool to define the strain distribution pattern and its evolution in the near-surface. These data are the basis to understand how the surface deformation build up. Consequently, they provide a picture of the characteristics of the principal slip zone at depth and is certainly of value for the identification and characterization of faults with potential for surface rupturing earthquakes.

[44] **Acknowledgments.** This research is supported by the European Commission Project "Relief": Large earthquake faulting and implications for seismic hazard assessment in Europe: The Izmit-Düzce earthquake sequence of 1999, Turkey, Mw 7.4, 7.1, EVG1-CT-2002-00069.

References

Akyüz, H. S., A. A. Barka, E. Altunel, R. D. Hartleb, and G. Sunal (2000), Field observations and slip distribution of the November 12, 1999 Düzce earthquake (M = 7.1), Bolu - Turkey, in *The 1999 Izmit and Düzce Earthquakes: Preliminary Results*, edited by A. A. Barka et al., pp. 63–70, Istanbul Tech. Univ., Istanbul.

Akyüz, H. S., R. D. Hartleb, A. A. Barka, E. Altunel, G. Sunal, B. Meyer, and R. Armijo (2002), Surface rupture and slip distribution of the 12 November 1999 Düzce earthquake (M7.1), North Anatolian Fault, Bolu, Turkey, *Bull. Seismol. Soc. Am.*, *92*, 61–66.

Ambraseys, N. N. (1970), Some characteristic features of the North Anatolian fault zone, *Tectonophysics*, *9*, 143–165.

Ambraseys, N. N. (2002), The seismic activity of the Marmara Sea region over the last 2000 years, *Bull. Seismol. Soc. Am.*, *92*, 1–18.

Ambraseys, N. N., and C. F. Finkel (1995), *The Seismicity of Turkey and Adjacent Areas: A Historical Review, 1500–1800*, 240 pp., Muhittin Salih Eren, Istanbul.

Armijo, R., B. Meyer, A. Hubert, and A. A. Barka (1999), Westward propagation of the North Anatolian fault into the northern Aegean: Timing and kinematics, *Geology*, *27*(3), 267–270.

Ayhan, M. A., C. Demir, A. Kilicoglu, I. Sanli, and S. M. Nakiboglu (1999), Crustal motion around the western segment of the north Anatolian fault zone: Geodetic measurements and geophysical interpretation, paper presented at IUGG99, Int. Union of Geodesy and Geophys., Birmingham, U. K.

Barka, A. A. (1981), Seismo-tectonic aspects of the North Anatolian fault zone, Ph.D. thesis, 335 pp., Univ. of Bristol, Bristol, U. K.

Barka, A. A. (1992), The North Anatolian fault zone, *Ann. Tecton.*, *6*, 164–195.

Barka, A. A. (1999), 17 August 1999 Izmit earthquake, *Science*, *285*, 1858–1859.

Barka, A. A., and P. L. Hancock (1984), Neotectonic deformation patterns in the convex-northwards arc of the North Anatolian fault, in *The Geological Evolution of the Eastern Mediterranean*, edited by J. G. Dixon and A. H. F. Robertson, *Geol. Soc. Spec. Publ.*, *17*, 763–773.

Barka, A. A., and K. Kadinski-Cade (1988), Strike-slip fault geometry in Turkey and its influence on earthquake activity, *Tectonophysics*, *7*, 663–684.

Barka, A. A., et al. (2000), The August 17, 1999 Izmit earthquake, M = 7.4, eastern Marmara region, Turkey: Study of surface rupture and slip distribution, in *The 1999 Izmit and Düzce Earthquakes: Preliminary Results*, edited by A. A. Barka et al., pp. 15–30, Istanbul Tech. Univ., Istanbul.

Barka, A. A., et al. (2002), The surface rupture and slip distribution of the August 17, 1999 Izmit earthquake, M = 7.4, North Anatolian Fault, *Bull. Seismol. Soc. Am.*, *92*, 43–60.

Burgmann, R., M. E. Ayhan, E. J. Fielding, T. J. Wright, S. McClusky, B. Aktug, C. Demir, O. Lenk, and A. Turkezer (2002), Deformation during the 12 November 1999 Düzce, Turkey, earthquake, from GPS and InSAR Data, *Bull. Seismol. Soc. Am.*, *92*, 161–171.

Cakir, Z., A. Barka, J. B. De Chabalier, R. Armijo, and B. Meyer (2003), Kinematics of the November 12, 1999 (Mw = 7.2) Düzce earthquake deduced from SAR interferometry, *Turk. J. Earth Sci.*, *12*, 105–118.

Canitez, N., and B. Ucer (1967), Computer determinations for the fault plane solutions in and near Anatolia, *Tectonophysics*, *4*, 235–244.

Hartleb, R. D., et al. (2002), Surface rupture and slip distribution along the Karadere segment of the 17 August 1999 Izmit and the western section of

the 12 November 1999 Düzce, Turkey, earthquakes, *Seismol. Soc. Am. Bull.*, *92*, 67–78.
Herece, E., and E. Akay (2003), 1:100.000 geological maps of the North Anatolian Fault, Appendix 3 and 4, Gen. Dir. of Miner. Res. and Explor., Ankara.
Hubert-Ferrari, A., R. Armijo, G. King, B. Meyer, and A. Barka (2002), Morphology, displacement, and slip rates along the northern Anatolian Fault, Turkey, *J. Geophys. Res.*, *107*(B10), 2235, doi:10.1029/2001JB000393.
Johnson, A. M., R. W. Fleming, and K. M. Cruikshank (1994), Shear zones formed along long, straight traces of fault zones during the 28 June 1992 Landers, California, earthquake, *Bull. Seismol. Soc. Am.*, *84*, 499–510.
Kahle, H.-G., M. Cocard, Y. Peter, A. Geiger, R. Reilinger, S. McClusky, R. King, A. Barka, and G. Veis (1999), The GPS strain rate field in the Aegean Sea and western Anatolia, *Geophys. Res. Lett.*, *26*(16), 2513–2516.
Kahle, H. G., M. Cocard, Y. Peter, A. Geiger, R. Reilinger, A. Barka, and G. Veis (2000), GPS-derived strain rate field within the boundary zones of the Eurasian, African, and Arabian Plates, *J. Geophys. Res.*, *105*(B3), 23,353–23,370.
Lazarte, C. A., J. D. Bray, A. M. Johnson, and R. E. Lemmer (1994), Surface breakage of the 1992 Landers earthquake and its effects on structures, *Bull. Seismol. Soc. Am.*, *84*, 547–561.
McClusky, S. C., et al. (2000), Global positioning system constraints on plate kinematics and dynamics in the eastern Mediterranean and Caucasus, *J. Geophys. Res.*, *105*(B3), 5695–5720.
McKenzie, D. P. (1972), Active tectonics of the Mediterranean region, *Geophys. J. R. Astron. Soc.*, *30*, 109–185.
Milkereit, C., et al. (2000), Preliminary aftershocks analysis of the Mw = 7.4 Izmit and Mw = 7.1 Düzce earthquake in western Turkey, in *The 1999 Izmit and Düzce Earthquakes: Preliminary Results*, edited by A. A. Barka et al., pp. 179–187, Istanbul Tech. Univ., Istanbul.
Muller, J. R., A. Aydin, and F. Maerten (2003), Investigating the transition between the 1967 Mudurnu Valley and 1999 Izmit earthquakes along the North Anatolian fault with static stress changes, *Geophys. J. Int.*, *154*, 471–482.
Naylor, M. A., G. Mandl, and C. H. K. Sijpesteijn (1986), Fault geometries in basement-induced wrench faulting under different initial stress states, *J. Struct. Geol.*, *8*(7), 737–752.
Özalaybey, S., M. Aktar, M. Ergün, H. Karabulut, M. Bouchon, C. Tapirdamaz, and A. Yoruk (2000), Aftershock studies following recent earthquakes in Turkey, paper presented at XXVII General Assembly, Eur. Seismol. Comm., Lisbon Univ., Lisbon, Portugal.
Reilinger, R. E., S. C. McClusky, M. B. Oral, W. King, and M. N. Toksöz (1997), Global positioning system measurements of present-day crustal movements in the Arabian-Africa-Eurasia plate collision zone, *J. Geophys. Res.*, *102*(B5), 9983–9999.
Reilinger, R. E., M. N. Toksöz, S. McClusky, and A. A. Barka (2000), 1999 Izmit, Turkey Earthquake was no surprise, *GSA Today*, *10*, 1–6.
Riedel, W. (1929), Zur mechanic geologischer brucherscheinungen, *Z. Min. Geol. Paleontol.*, 1929, Suppl. B, 354–368.
Şaroğlu, F., Ö. Emre, and İ. Kuşçu (1992), Active fault map of Turkey, map, Gen. Dir. of Miner. Res. and Explor., Ankara.
Şengör, A. M. C. (1979), The North Anatolian transform fault: Its age, offset and tectonic significance, *J. Geol. Soc.*, *136*, 269–282.
Seymen, I. (1975), Tectonic characteristics of the North Anatolian fault zone in the Kelkit valley, Ph.D. thesis, 192 pp., Istanbul Tech. Univ., Istanbul.
Sibson, R. H. (2003), Thickness of the seismic slip zone, *Bull Seismol. Soc. Am.*, *93*(3), 1169–1178.
Sieh, K. L., et al. (1993), Near-field investigations of the Landers earthquake sequence, April to July, 1992, *Science*, *260*, 171–176.
Straub, C., H. G. Kahle, and C. Schindler (1997), GPS and geologic estimates of the tectonic activity in the Marmara Sea region, NW Anatolia, *J. Geophys. Res.*, *102*(B12), 27,587–27,601.
Tchalenko, J. S. (1970), Similarities between shear zones of different magnitudes, *Geol. Soc. Am. Bull.*, *81*, 1625–1639.
Tchalenko, J. S., and N. N. Ambraseys (1970), Structural analysis of the Dasht-e Bayaz, Iran, earthquake fractures, *Geol. Soc. Am. Bull.*, *81*, 41–60.
Tchalenko, J. S., and M. Berberian (1975), Dasht-e Bayaz fault, Iran: Earthquake and earlier related structures in bedrock, *Geol. Soc. Am. Bull.*, *86*, 703–709.
Tibi, R., G. Bock, Y. Xia, M. Baumbach, H. Grosser, C. Milkereit, S. Karakisa, S. Zunbul, R. Kind, and J. Zschau (2001), Rupture processes of the 1999 August 17 Izmit and November 12 Düzce (Turkey) earthquakes, *Geophys. J. Int.*, *144*, F1–F7.
Tokay, M. (1973), Geological observation on the North Anatolian fault zone between Gerede and Ilgaz, paper presented at Symposium on the North Anatolian Fault Zone and Earthquake Belt, Miner. Res. and Explor. Inst. of Turkey, Ankara.
Utkucu, M., S. S. Nalbant, J. McCloskey, S. Steacy, and O. Alptekin (2003), Slip distribution and stress changes associated with the 1999 November 12, Düzce (Turkey), *Geophys. J. Int.*, *153*, 229–241.
Westaway, R. (1994), Present-day kinematics of the middle-east and eastern Mediterranean, *J. Geophys. Res.*, *99*(B6), 12,071–12,090.
Wilcox, R. E., T. P. Harding, and D. R. Seely (1973), Basic wrench tectonics, *AAPG Bull*, *57*(1), 74–96.
Woodcock, N. H., and C. Schubert (1994), Continental strike-slip tectonics, in *Continental Deformation*, edited by P. L. Hancock, pp. 251–263, Elsevier, New York.

M. Barchi, Dipartimento di Scienze della Terra, Universita' degli Studi di Perugia, I-06100 Perugia, Italy. (mbarchi@unipg.it)
N. Palyvos, D. Pantosti, and S. Pucci, Sismologia e Tettonofisica, Istituto Nazionale di Geofisica e Vulcanologia, Via di Vigna Murata, 605, I-00143 Rome, Italy. (palyvos@ingv.it; pantosti@ingv.it; pucci@ingv.it)
C. Zabci, Istanbul Technical University, Ayaza a Kampüsü, 80626 Maslak, Istanbul, Turkey. (zabci@itu.edu.tr)